Ammonium Dinitramide: Kinetics and Mechanism of Thermal Decomposition

Sergey Vyazovkin and Charles A. Wight*

Department of Chemistry, University of Utah, Salt Lake City, Utah 84112

Received: August 19, 1996; In Final Form: April 15, 1997[⊗]

Thermal decomposition of ammonium dinitramide (ADN) has been studied by differential scanning calorimetry (DSC) and thermal gravimetry combined with mass spectrometry (TG−MS). ADN decomposes in the range 130−230 °C with an overall heat release of 240 ± 40 kJ mol^{-1}. The product gases have been identified by MS as NH_3, H_2O, NO, N_2O, NO_2, HONO, and HNO_3. The global activation energy determined from TG experiments decreases from 175 ± 20 kJ mol^{-1} at the beginning of the reaction to 125 ± 20 kJ mol^{-1} when the reaction is near completion. Experiments conducted at different carrier gas flow rates indicate that the reaction is catalyzed by product gases released during the reaction. A condensed phase ionic reaction mechanism is proposed, in which ammonium nitrate and ammonium mononitramide (NH_4NNO_2) are formed as intermediates in two competing channels.

Introduction

Ammonium dinitramide (ADN) is a powerful oxidizer that is a potential halogen-free replacement for ammonium perchlorate in solid rocket propellants. This has inspired interest in understanding the kinetics and mechanism of its thermal decomposition. A qualitative study of ADN thermal decomposition based on mass spectroscopic measurements[1] was reported in 1993. At about the same time, Brill and co-workers used a T-jump/FTIR method to study ADN decomposition,[2] and they have proposed a mechanism for gas phase decomposition that involves two main branches,

$$NH_4N(NO_2)_2 \rightarrow NH_3 + HNO_3 + N_2O \quad (1)$$

$$NH_4N(NO_2)_2 \rightarrow NH_3 + HN(NO_2)_2 \quad (2)$$

These steps are analogous to the accepted decomposition mechanisms of ammonium perchlorate and ammonium nitrate (AN), both of which are initiated by dissociative vaporization to form ammonia and the corresponding strong acid. Reaction 1 is mildly endothermic and is the only proposed source of nitric acid in this scheme. Reaction 2 is followed by decomposition of dinitramidic acid, $HN(NO_2)_2$, and the overall conversion to products was proposed to be

$$12NH_4N(NO_2)_2 \rightarrow 3NH_3 + 10N_2O + 6NO_2 + 15H_2O + 2NO + 6N_2 + HNO_3 + 2NH_4NO_3 \quad (3)$$

The aforementioned studies were carried out at either low pressures[1] or at high temperatures,[2] which are conditions that favor a gas phase decomposition mechanism. No kinetic parameters were given in either paper.

In recent reports, Russell and co-workers have reported that condensed phase thermal decomposition of ADN proceeds via two pathways. Below 130 °C, ADN is converted to AN by elimination of N_2O. At higher temperatures, evidence of N−N bond scission forming NO_2 has been observed.[3] Two polymorphs of crystalline ADN have been observed, both of which undergo irreversible thermal decomposition at the melting point.[4] The results of Russell and co-workers suggested that a low-temperature ionic decomposition mechanism may exist for ADN that does not involve initial formation of ammonia and dinitramidic acid.

The purpose of our current study is to investigate the condensed phase thermal decomposition of ADN. The emphasis of the work is on the kinetics and mechanism of the process studied by DSC and TG−MS technique. Conditions favoring condensed phase decomposition have been established by performing experiments at atmospheric pressure and low temperature (i.e., slow heating rates). Some preliminary kinetic experiments have been presented in a preliminary report.[5] This paper gives expanded results and a complete kinetic analysis. In an accompanying paper, Oxley *et al.*[6] report their studies of thermal decomposition of ADN and its ^{15}N and ^{2}H isotopomers. The experimental techniques used in our two studies are different, providing complementary experimental accounts of the same physical process.

Experimental Section

A 1 g sample of crystalline ADN was kindly supplied by Thiokol Corp. It was stored at room temperature in the dark (to avoid photochemical degradation) and was used in our experiments as supplied with no further purification.

Five DSC experiments were performed using a TA Instruments Model DSC-2910 modulated differential scanning calorimeter. Indium was used as a calibration standard. Samples of ADN (∼0.6 mg) were placed into aluminum pans that were closed but not sealed (to avoid buildup of excessive gas pressures during decomposition). The samples were heated at rates of 2, 5, or 10 °C min^{-1} in a flowing nitrogen atmosphere (100 mL min^{-1}).

Three series of five TG experiments each were run on a Rheometrics Model 1000M+ at nitrogen carrier gas flow rates of 30, 100, and 150 mL min^{-1}. Samples of ADN (∼0.6 mg) were placed in open aluminum foil pans and heated at temperature-programmed rates from 1 to 20 °C min^{-1}.

Five TG−MS experiments were performed on a Perkin-Elmer TGS-2 coupled with a quadrupole mass spectrometer (Extranuclear Laboratories, Inc., Model SpectrEL). Samples (∼2 mg) were decomposed in open aluminum pans under flowing argon (100 mL min^{-1}) carrier gas. The evolved gases were sampled continuously by the mass spectrometer, where they were ionized in a 12 eV electron impact ion source. This instrument provides simultaneous monitoring of the mass loss of the sample and

[⊗] Abstract published in *Advance ACS Abstracts,* June 15, 1997.

S1089-5639(96)02547-9 CCC: $14.00

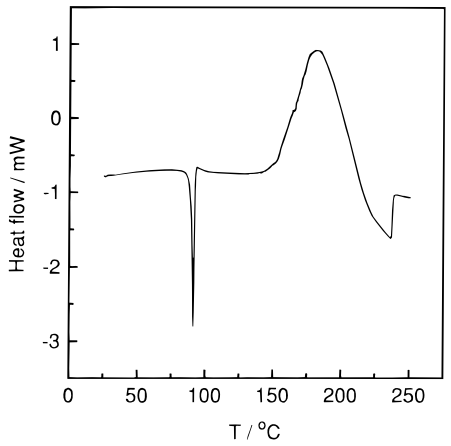

Figure 1. DSC trace of the thermal transformation of ADN at heating rate 5 °C min^{-1}.

the formation of positive ions in the range 10−250 amu. Based on the carrier gas flow rate, the time between gas formation and detection in the mass spectrometer is approximately 1 s. During each experiment, a complete mass spectrum was collected every 3−5 s. The low ionization potential was used in order to avoid ionizing the argon carrier gas and to minimize fragmentation of the reaction product ions in the ion source. One experiment was performed in which the electron energy in the ion source was set to 14.5 eV in order to maximize the sensitivity for detecting any O_2 and N_2 that might be formed in the decomposition reaction.

Results

Differential Scanning Calorimetry. A typical DSC curve is shown in Figure 1, demonstrating heat transfer to and from the ADN sample during the heating cycle. The endotherm at 92 °C corresponds to the melting temperature of our ADN sample. Russell *et al.*[4] report that the melting point of pure ADN may be as high as 95 °C. If this is correct, then the lower temperature of our melting endotherm indicates that we may have as much as 3% impurity in our sample, most likely AN. The molten liquid ADN undergoes thermal decomposition over the temperature range 130−230 °C. The process is highly exothermic, and the integrated heat release in three experiments was measured to be 1.923, 1.921, and 2.029 kJ/g for an average value of 1.96 ± 0.35 kJ g^{-1} or 240 ± 40 kJ mol^{-1}. The exotherm is followed by a small endotherm near 235 °C. This could be due to a cooling effect caused by adiabatic expansion of gases escaping the aluminum pans, or possibly by vaporization of water from the decomposition reaction. A similar endotherm was observed by Oxley *et al.* in their DSC runs that were performed in sealed glass tubes.[6] No solid residue was found in the pans after the thermal decomposition cycle.

Thermal Gravimetric Analysis. Data from three typical TG experiments conducted on the Rheometrics instrument are shown in Figure 2. All three runs were carried out at a heating rate of 4 °C min^{-1}, but different N_2 carrier gas flow rates (30, 100, and 150 mL min^{-1}). The mass loss (formation of product gases) takes place over approximately the same temperature range as the heat release observed in the DSC experiments. Note that the TG results obtained at high carrier flow rates exhibit a shift of the decomposition reaction to slightly higher temperatures. At each of the three carrier gas flow rates, a series of five experiments were performed at different heating rates in order to determine the activation energy for the global thermal decomposition reaction as a function of the extent of reaction. The isoconversional method used to determine the activation energy is described in the next section.

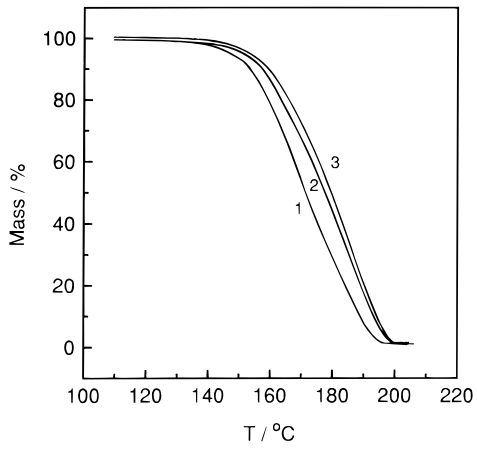

Figure 2. TG traces of the thermal decomposition of ADN at the same heating rate (4 °C min^{-1}) but different N_2 carrier gas flow rates: (1) 30 mL min^{-1}; (2) 100 mL min^{-1}; (3) 150 mL min^{-1}.

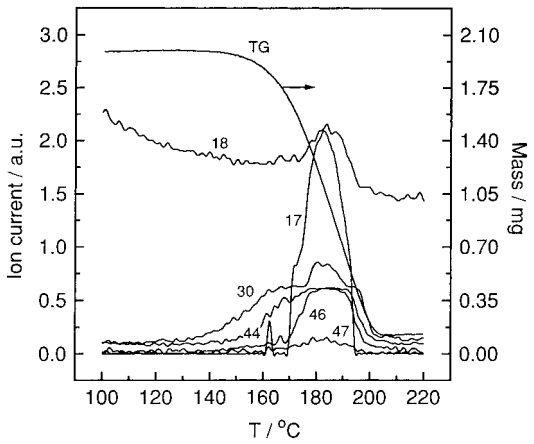

Figure 3. Results of TG-MS experiment at 5 °C min^{-1}. The numbers correspond to the mass-to-charge ratio of ions detected from the gaseous products. TG curve, right-hand ordinate.

Five TG−MS experiments were performed using the Perkin-Elmer instrument. The TG traces were comparable to the results obtained with the Rheometrics instrument. However, a detailed kinetic analysis was not performed.

Analysis of Evolved Gases by Mass Spectrometry. Analysis of the gases evolved during decomposition reveals the formation of ions having a mass to charge ratio of 17, 18, 30, 44, 46, 47, and 63 amu, as illustrated in Figure 3. Because ADN contains only hydrogen, nitrogen, and oxygen, the ions are unambiguously identified as NH_3, H_2O, NO, N_2O, NO_2, HONO, and HNO_3. The complete mass spectra were examined, and no other reaction products were detected. That is, at all other masses in the range 10−250 amu, the ion signal was either insignificant or was constant during the course of the reaction (e.g., mass 28 due to background N_2 or CO). The absence of noise in the mass 17 channel at temperatures below 160 °C is due to interference with the adjacent channel at 18 amu. The data analysis software assigns a value of zero for the mass 17 channel unless it can resolve a separate peak at this mass. Figure 3 shows that the temperature range of product gas evolution corresponds to the mass loss from the sample. There is an apparent transient burst that appears in the mass 17 data channel corresponding to transient emission of NH_3. This feature was not reproducible, but appeared in two of the five TG−MS experiments performed. The cause of the feature remains unclear.

The formation of gaseous reaction products appears to occur in two distinct stages. The first products detected are N_2O, NO,

and NO_2 (Figure 3). They are followed at a later stage by H_2O, HONO, NH_3, and HNO_3. Whereas HONO was not reported in the previous MS study,[1] this product has been detected by FTIR technique as a product of UV photolysis.[7] Also, the MS experiments[1] were not able to firmly establish whether water is a product of thermal decomposition. The present data show that while water is present in the background gases, it is also formed as a reaction product in the late stages of ADN decomposition.

The TG−MS experiments are normally performed with the electron impact ion source operating at 12.0 eV. This is to avoid ionization of the argon carrier gas. One experiment was performed at 14.5 eV in order to increase the sensitivity for detecting N_2 and O_2. Although ions at masses 28 and 32 amu were detected (due to ionization of background gases), no evidence was found for formation of O_2 or N_2 from thermal decomposition of ADN under the experimental conditions of this study. The most significant difference in the results obtained by increasing the ionization potential to 14.5 eV is a decrease in the magnitude of the ion signal at 46 amu (NO_2^+) and a corresponding increase at 30 amu (NO^+). We therefore concluded that much of the NO^+ arises from fragmentation of NO_2^+ in the ion source, particularly in the early stages of the reaction. Some NO is undoubtedly formed in the reaction, because ion signals at 30 and 46 amu do not have exactly the same dependence on temperature (c.f., Figure 3). However, the amount of NO observed is undoubtedly less than that suggested by the magnitude of the ion signal at 30 amu.

Kinetic Analysis of TG Data

The TG data have been analyzed to determine the temperature dependence of the thermal decomposition rate constant (activation energy) as well as the reaction model (dependence of reaction rate on the extent of conversion to products),

$$\frac{d\alpha}{d\tau} = k(T)\, f(\alpha) = A \exp\left(\frac{-E_A}{RT}\right) f(\alpha) \qquad (4)$$

where T is the temperature; t is the time; α is the extent of reaction; $k(T)$ is the rate constant; $f(\alpha)$ is the reaction model; A is the pre-exponential factor; E_A is the activation energy; and R is the gas constant. For experiments carried out at constant heating rate,

$$\beta = \frac{dT}{dt} = \text{constant} \qquad (5)$$

eq 4 can be rearranged and integrated to obtain

$$g(\alpha) = \int_0^\alpha [f(\alpha')]^{-1}\, d\alpha' = (A/\beta)\int_0^T \exp(-E_A/RT')\, dT' = \frac{A}{\beta} I(T) \qquad (6)$$

which is the integrated form of the reaction model that is normally used to describe the kinetics of reactions in solids.[8,9] Several examples of reaction models and their integrated forms are given in Table 1. Note that the integral $I(T)$ is a function of temperature but depends parametrically on E_A.

A common practice is to assume a particular reaction model (e.g., first-order reaction), solve eq 6 for $\alpha(T)$, and evaluate the Arrhenius parameters by fitting the kinetic equation to the experimental data. However, this procedure cannot yield trustworthy values of E_A and A for two reasons. First, this model-fitting method yields only a single activation energy for the reaction. However, E_A may actually vary during the course of the reaction, and the model-fitting method cannot be used to extract this information. Second, unless the reaction model can be determined by some independent means, it is often difficult to distinguish between models on the basis of fits to the experimental data. To illustrate this, we performed fits of our TG data to the 13 different reaction models listed in Table 1 using the Coats−Redfern method.[10] The results of the fits for a typical experiment are shown in Table 2. Based on a statistical analysis[11] of correlation coefficients, the four best models (6, 9, 10, and 11) are indistinguishable. In other words, there is no statistical basis for choosing any one of them over the others.

To overcome the limitations of the model-fitting method, we have determined the activation energy as a function of α by use of a nonlinear isoconversional method[12] that is model-independent. This method makes the simple assumption that the integrated form of the reaction model, $g(\alpha)$, does not depend on the heating rate, β. According to eq 6, for any particular value of α, the value of $I(T)/\beta$ should be independent of the heating rate, β. Therefore, if n experiments are performed at different heating rates, the optimal value of E_A can be found[12] at any chosen value of α by minimizing the function

$$|n(n-1) - \sum_i^n \sum_{j\neq i}^n \frac{I(T_i)}{\beta_i}\frac{\beta_j}{I(T_j)}| \qquad (7)$$

with respect to E_A, which is a parameter in the function $I(T)$. The minimization procedure is repeated for different extents of conversion to determine the value of E_A as a function of α.

This analysis was performed for the series of 15 TG experiments carried out on the Rheometrics instrument. At each value of the carrier gas flow rate, the values of $T(\alpha)$ were

TABLE 1: Set of Alternate Reaction Models Applied To Describe the Reaction Kinetics in Heterogeneous Solid State Systems (Adapted from Refs 8 and 9)

N	reaction model	$f(\alpha)$	$g(\alpha)$
1	power law	$4\alpha^{3/4}$	$\alpha^{1/4}$
2	power law	$3\alpha^{2/3}$	$\alpha^{1/3}$
3	power law	$2\alpha^{1/2}$	$\alpha^{1/2}$
4	power law	$2/3\alpha^{-1/2}$	$\alpha^{3/2}$
5	one-dimensional diffusion	$1/2\alpha^{-1}$	α^2
6	Mampel (first order)	$1-\alpha$	$-\ln(1-\alpha)$
7	Avrami−Erofeev	$4(1-\alpha)[-\ln(1-\alpha)]^{3/4}$	$[-\ln(1-\alpha)]^{1/4}$
8	Avrami−Erofeev	$3(1-\alpha)[-\ln(1-\alpha)]^{2/3}$	$[-\ln(1-\alpha)]^{1/3}$
9	Avrami−Erofeev	$2(1-\alpha)[-\ln(1-\alpha)]^{1/2}$	$[-\ln(1-\alpha)]^{1/2}$
10	three-dimensional diffusion	$2(1-\alpha)^{2/3}(1-(1-\alpha)^{1/3})^{-1}$	$[1-(1-\alpha)^{1/3}]^2$
11	contracting sphere	$3(1-\alpha)^{2/3}$	$1-(1-\alpha)^{1/3}$
12	contracting cylinder	$2(1-\alpha)^{1/2}$	$1-(1-\alpha)^{1/2}$
13	second order	$(1-\alpha)^2$	$(1-\alpha)^{-1}-1$

TABLE 2: Arrhenius Parameters Computed for the Thermal Decomposition of ADN at 5.5 °C min^{-1} (Carrier Gas Flow Rate 100 mL min^{-1})

N	E/kJ mol^{-1}	log(A/min^{-1})	$-r$
1	24.5	1.7	0.9783
2	35.1	3.0	0.9813
3	56.2	5.5	0.9837
4	182.9	20.1	0.9862
5	246.2	27.3	0.9865
6[a]	139.4	15.5	0.9928
7	29.5	2.4	0.9903
8	41.7	3.9	0.9913
9[a]	66.1	6.9	0.9921
10[a]	269.1	29.3	0.9928
11[a]	131.0	13.9	0.9924
12	127.6	13.6	0.9910
13	177.8	20.5	0.9436

[a] Statistically equivalent values.

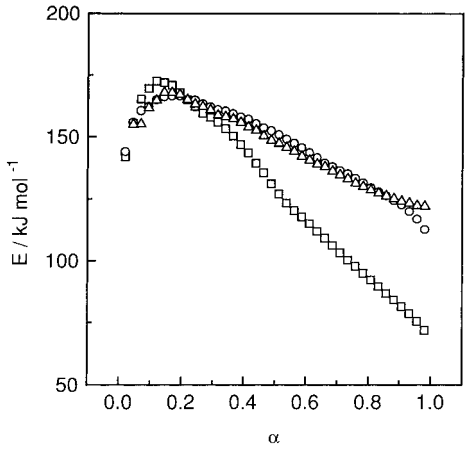

Figure 4. Dependence of the activation energy on conversion for the thermal decomposition of ADN at different carrier gas flow rates (squares, 30 mL min^{-1}; circles, 100 mL min^{-1}; triangles, 150 mL min^{-1}).

tabulated for 40 values of α in the range 0.02−0.99 for five experiments performed at different heating rates. The resulting dependence of E_A on α is shown in Figure 4.

At the lowest flow rate (30 mL min^{-1}), the activation energy exhibits a marked decrease with the extent of reaction, from 175 ± 20 to 75 ± 20 kJ mol^{-1} near the end of the reaction. At intermediate flow rates (100 mL min^{-1}), the activation energy starts at about the same value (175 ± 20 kJ mol^{-1}), but decreases only to 125 ± 20 kJ mol^{-1} at the completion of the reaction. Experiments carried out at the highest N_2 flow rate (150 mL min^{-1}) showed essentially the same results as intermediate flow rates.

The results obtained in our preliminary study[5] were based on three TG experiments that were performed at different heating rates but constant carrier gas flow rate (100 mL min^{-1}) using a different instrument. Due to differences in the geometry of the sample chamber, the carrier gas flow rates are not directly comparable with those of the Rheometrics instrument. Kinetic analysis of the previous results gave a somewhat higher value of the activation energy (200 ± 20 kJ mol^{-1}), which was nearly constant throughout the reaction.[5] The results reported in this paper are based on a much larger number of experiments. In the accompanying paper, Oxley *et al.* report that the activation energy for ADN decomposition (based on the model fitting method) is 155 kJ mol^{-1}.[6]

Discussion

Heat Release. Our DSC experiments show that the heat released during thermal decomposition of ADN is 240 ± 40 kJ mol^{-1}. The net reaction (3) as written by Brill and co-workers[2] for the high-temperature mode of decomposition has been estimated to be exothermic by 113 kJ mol^{-1}. Our value is more than twice as large, which is indicative of a much greater extent of conversion to thermodynamically favored products. Our measurement of the heat release is in agreement with that of Oxley *et al.* (211 kJ mol^{-1})[6] despite the fact that their experiments were conducted in sealed glass tubes and ours were in unsealed aluminum pans. Based on this agreement, we conclude that the extent of reaction is essentially complete in both experiments. That is, the escape of endothermic gaseous products such as vaporized ADN or $NH_3 + HN(NO_2)_2$ is minimized.

Product Analysis. In the Introduction of this paper, we suggested that the experimental conditions of the previously reported MS[1] and T-jump/FTIR[2] experiments probably favored a gas phase decomposition mechanism, whereas our experiments (and those of Russell *et al.*),[3] which are carried out at significantly lower temperatures and higher pressures, probably favor a condensed phase reaction mechanism. It is the comparison of reaction product distributions in the various experiments that provides the most compelling evidence for this conclusion. In this section we make some key comparisons of our results with the previous experiments and note a few key observations that provide important clues to the nature of the mechanism of condensed phase thermal decomposition of ADN.

The previously reported products of gas phase decomposition by MS[1] are NH_3, N_2O, and some NO, which appear simultaneously at 90 °C. At higher temperatures (150 °C) NH_3 and N_2O are still the dominant products, but the relative concentrations of NO, H_2O, and NO_2 increase until they are of comparable magnitude to NH_3 and N_2O at about 170 °C. The first products detected by T-jump/FTIR method[2] are mostly NH_3, HNO_3, and N_2O, which are formed in roughly equal amounts. The concentration of N_2O increases during the decomposition. Smaller amounts of NO_2 and NH_4NO_3 were also detected. In our experiments, which are conducted under conditions favoring a condensed phase mechanism, the nitrogen oxides (NO, N_2O, NO_2) were detected as early products. However, the most striking difference between our results and the previous "gas phase" decomposition experiments is that we do not detect any NH_3 until relatively late in the decomposition process (Figure 3).

Another major difference between our results and the conclusions of previous studies concerns the role of nitric acid in the mechanism. Based on the previous experiments,[1,2] the gas phase thermal decomposition of ADN proceeds at least partly as a result of reaction 1, even though nitric acid was detected only as a minor product. Our condensed phase experiments detected nitric acid only at the highest heating rate (10 °C min^{-1}) and in a very low amount (less than 5% of any of the nitrogen oxides). The low concentration of HNO_3 observed in other experiments was rationalized[1] by the fact that nitric acid undergoes heterogeneous decomposition on the walls of the vacuum chamber. However, this explanation is doubtful because the decomposition of nitric acid inevitably gives rise to the formation of oxygen,[1] which has never been detected as a reaction product. We made a careful search for O_2 in our TG−MS experiments and were unable to detect its formation. On this basis, we conclude that under our experimental conditions (slow heating rates and pressures near 1 atm), reaction 1 plays an insignificant role in the decomposition mechanism.

Our data have also shown no evidence for the production of N_2 during the experiment. Similarly, nitrogen has not been reported in the other MS study.[1] On this basis, we conclude that the conversion of ammonia to nitrogen

$$NH_3 + OH \rightarrow H_2O + NH_2 \quad (8)$$

$$NH_2 + NO \rightarrow N_2 + H_2O \quad (9)$$

which was proposed[2] as a part of the overall reaction 3 cannot be occurring to any significant extent under our conditions. However, we note that under experimental conditions where gases are confined in the reaction vessel, formation of N_2 has been observed,[6,16] and the isotopic labeling studies show that one N atom originates from the ammonium ion, whereas the other originates on an NO_2 group in the parent ADN molecule. Brower *et al.* reported that N_2 is formed in a side reaction during AN decomposition in sealed glass tubes,[16] so the formation of N_2 from ADN under similar conditions is consistent with formation of AN as an intermediate in the thermal decomposition of ADN.

The dinitramidic acid, $HN(NO_2)_2$, product in reaction 2 was not detected directly in Brill's T-jump/FTIR experiments.[2] This molecule is claimed to have been monitored by $m/e = 46$ (NO_2^+) and 60 (NNO_2^+) in the earlier MS study,[1] presumably as a result of parent ion fragmentation. However, the relative abundance of the two ions seemed to be poorly correlated. In our study, we detected the NO_2^+ ion, but not NNO_2^+. This suggests that these ions arise from different neutral species and may actually arise from direct ionization of NO_2 (and possibly NNO_2) decomposition products. Overall, our experiment provides no evidence for the formation of dinitramidic acid, especially via (2) because no NH_3 was detected in the early stages of decomposition.

An Ion−Molecule Reaction Mechanism for Condensed Phase ADN Decomposition. The fact that we have detected no NH_3 in the early stages of ADN decomposition makes it extremely unlikely that reactions 1 and 2 play a significant role in the mechanism. Instead, we suggest that decomposition in the molten salt (recall that ADN melts at 92 °C) follows an ionic mechanism involving formation of other ammonium salts such as ammonium nitrate. By analogy with (1) we propose that one channel of ADN decomposition is oxygen transfer from one NO_2 group to the N atom of another NO_2 group followed by dissociation of an N−N bond

$$NH_4N(NO_2)_2 \rightarrow N_2O + NH_4^+ + NO_3^- \qquad (10)$$

This pathway is consistent with the recent reports by Russell and co-workers.[3,4] Ammonium nitrate is reported[13−16] to decompose to $N_2O + 2\ H_2O$ via a mechanism involving formation of ammonia and nitric acid as intermediates. Therefore, reaction 10 cannot account for our observations of NO and NO_2 early in the decomposition prior to the appearance of NH_3. We propose that second channel of the decomposition begins with N−N bond rupture and the formation of nitrogen dioxide and mononitramide ion:

$$NH_4N(NO_2)_2 \rightarrow NO_2 + NH_4^+ + NNO_2^- \qquad (11)$$

There have been several theoretical studies that report bond dissociation energies in $HN(NO_2)_2$ and $NH_4N(NO_2)_2$. Considering homolytic and heterolytic ruptures of the H−N and N−N bonds, it has been calculated that the lowest energy pathway is homolytic bond cleavage to give $HNNO_2$ and NO_2 radicals, which requires 184 kJ mol^{-1}.[17] Some other estimates of the N−N bond dissociation energy are 202,[18] 204,[19] and 124−197 kJ mol^{-1}.[20] Therefore, our experimental value of the initial activation energy 175 ± 20 kJ mol^{-1} is consistent with an initial step in the reaction which involves N−N bond scission.

Further support for the role of reaction 11 comes from flowing afterglow studies[21] which have shown that the main pathway for collision-induced dissociation of gas phase dinitramide ion is

$$N(NO_2)_2^- \rightarrow NNO_2^- + NO_2 \qquad (12)$$

The mononitramide ion (NNO_2^-) undergoes several tautomeric transformations[22] and dissociates via

$$NNO_2^- \rightarrow NO^- + NO \qquad (13)$$

The net reaction for processes 11−13 is

$$NH_4N(NO_2)_2 \rightarrow NH_4^+ + NO_2 + NO^- + NO \qquad (14)$$

The electron affinities of NO_2 and NO are nearly identical,[23] so the net process

$$NH_4N(NO_2)_2 \rightarrow NH_4^+ + NO_2^- + 2NO \qquad (15)$$

should be competitive. This scheme predicts that both NO and NO_2 should be formed, but the $m/e = 30$ ion should be more abundant than $m/e = 46$ (Figure 3) in the early stages of decomposition because NO_2 is detected in the mass spectrometer predominantly as NO^+.[24] Also, proton transfer to NO_2^- could explain the presence of HONO in the mass spectra of reaction products (Figure 3).

Figure 3 shows that ammonia and water are formed in the late stages of the reaction. The most likely source of these products is the thermal decomposition of ammonium nitrate, which has been discussed in detail by Brower *et al.*[16] According to their study, AN decomposes by an ionic mechanism below 290 °C, which gives way to a free radical mechanism at higher temperatures. Their scheme includes NH_3 as a key intermediate and gives H_2O and N_2O as the net reaction products, which is entirely consistent with our observations for ADN.

Reaction Kinetics. The kinetic analysis of our TG experiments by the isoconversional method revealed that the activation energy decreases during the thermal decomposition reaction from an initial value near 175 ± 20 kJ to 125 ± 20 kJ mol^{-1} near the end of the reaction. According to our proposed mechanism, the initial steps in the reaction should be elimination of N_2O from the dinitramide anion in ADN, reaction 10, or scission of one of the N−N bonds in dinitramide, reaction 11. The potential energy barrier for reaction 10 is not known; however, the calculated N−N bond dissociation energy in dinitramide is consistent with our initial activation energy of 175 ± 20 kJ mol^{-1}, as mentioned previously.

The reduction in activation energy with the extent of reaction is consistent with two other observations. First, the activation energy of AN decomposition at temperatures near 200 °C is reported to be 118 kJ mol^{-1}.[16] Therefore, a reaction that occurs primarily by conversion of ADN to AN would be expected to exhibit a decrease in E_A in this temperature range. Second, the thermal decomposition of AN is known to be catalyzed by NO_2,[25,26] which we have shown is one of the initial decomposition products of ADN. Indirect evidence for this is shown in Figure 4, which shows that the decrease in activation energy is less pronounced at high carrier gas flow rates. The most likely cause of this effect is that autocatalytic gases such as NO_2 are more effectively removed from the reaction system at high carrier gas flow rates.

The isoconversional method of kinetic analysis does not, by itself, permit an analysis of the Arrhenius pre-exponential factor and the reaction model. However, the reaction model can be reconstructed by a method that makes use of an artificial isokinetic relationship.[27,28] Using this method, we have numerically evaluated the integrated form of the reaction model, $g(\alpha)$ in eq 6, taking into account the experimentally determined variation of E_A with α. Figure 5 shows a comparison of $g(\alpha)$ obtained from the Rheometrics TG data (at 100 mL min^{-1} N_2 flow) with the reaction models listed in Table 1. The closest match is to model number 6 (first-order kinetic model), although some deviation is observed for $\alpha > 0.7$. Interestingly, the agreement with models 9, 10 and 11 is obviously worse, even though the model-fitting method was unable to distinguish between them.

Our kinetic results are essentially in agreement with Oxley *et al.*, who report that the reaction exhibits first-order kinetics with an activation energy of 155 kJ mol^{-1},[6] which is nearly an average value obtained in our experiments. However, we are convinced that the isoconversional method is superior for its

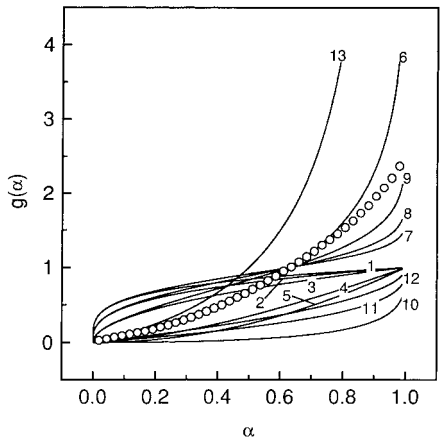

Figure 5. Dependence $g(\alpha)$ for the models shown in Table 1 (solid curves) and for the experimental data (circles).

ability to extract reliable kinetic parameters from the data. It provides the additional advantage of detecting changes in activation energy with the extent of reaction, which can reveal the effect of forming autocatalytic gases such as NO_2.

Conclusions

Kinetic analysis performed by the isoconversional method on thermogravimetric data has shown that thermal decomposition of ADN has an initial overall activation energy of 175 ± 20 kJ mol^{-1}. This decreases with the extent of conversion to about 125 ± 20 kJ mol^{-1} at the end of the reaction. The decrease in activation energy depends on the carrier gas flow rate. The initial value is consistent with theoretical estimates of the energy of the N−N bond dissociation energy in ADN and dinitramidic acid. The mechanism of condensed phase thermal decomposition of ADN has been found to be different from the dissociative vaporization that occurs in the gas phase. This conclusion is based largely on the fact that ammonia is not detected until the late stages of reaction. We propose that condensed phase ADN decomposes predominantly by an ionic mechanism with the formation of ammonium salts instead of ammonia. Our proposed mechanism explains the formation of nitrogen oxides (NO, NO_2, N_2O) in the early stages of decomposition (below about 170 °C). In the late stages of decomposition, gassification of the remaining ammonium salts results in formation of ammonia and water by a combination of ionic and free radical reactions.

Acknowledgment. This research is supported by the Office of Naval Research under contract No. N00014-95-1339. We are grateful to Dr. Robert Wardle of Thiokol Corporation for providing the sample of ADN.

References and Notes

(1) Rossi, M. J.; Bottaro, J. C.; McMillen, D. F. *Int. J. Chem. Kinet.* **1993**, *25*, 549.
(2) Brill, T. B.; Brush, P. J.; Patil, D. G. *Combust. Flame* **1993**, *92*, 178.
(3) Russell, T. P.; Stern, A. G.; Koppes; W. M.; Bedford, D. C. CPIA Publication, Proceedings of the JANNAF Combustion Meeting, Hampton, VA, Oct 19−23, 1992 5646.
(4) Russell, T. P.; Piermarini, G. J.; Block, S.; Miller, P. J. *J. Phys. Chem.* **1996**, *100*, 3248.
(5) Wight, C. A.; Vyazovkin, S. Proceedings of the JANNAF Combustion Subcommittee Meeting, Monterey, CA, November, 1996.
(6) Oxley, J. C.; Smith, J. L.; Zheng, W.; Rogers, E.; Coburn, M. D. *J. Phys. Chem.* **1997**, *101*, xxx.
(7) Snelson, A.; Tulis, A. J.; Heberlein, D. C.; Patel, D. L. *Proc. Int. Pyrotech. Semin.* **1994**, *19*, 531.
(8) Brown, M. E.; Dollimore, D.; Galwey, A. K. *Reactions in the Solid State, Comprehensive Chemical Kinetics*; (Elsevier: Amsterdam, 1980; Vol. 22.
(9) Sestak, J. *Thermophysical Properties of Solids, Comprehensive Analytical Chemistry*; Elsevier: Amsterdam, 1984; Vol. 12 D.
(10) Coats, A. W.; Redfern, J. P. *Nature* **1964**, *201*, 68.
(11) Johnson, N. L.; Leone, F. C. *Statistics and Experimental Design in Engineering and the Physical Sciences*; Wiley & Sons: New York, 1977.
(12) Vyazovkin, S.; Dollimore, D. *J. Chem. Inf. Comput. Sci.* **1996**, *36*, 42.
(13) Friedman, L.; Bigeleisen, J. *J. Chem. Phys.* **1950**, *18*, 1325.
(14) Rosser, W. A.; Enami, S. H.; Wise, H. *J. Phys. Chem.* **1963**, *67*, 1753.
(15) Saunders, H. L. *J. Chem. Soc.* **1922**, *121*, 698.
(16) Brower, K. R.; Oxley, J. C.; Tewari, M. *J. Phys. Chem.* **1989**, *93*, 4029.
(17) Politzer, P.; Seminario, J. M. *Chem. Phys. Lett.* **1993**, *216*, 348.
(18) Seminario, J. M.; Politzer, P. *Int. J. Quantum Chem., Symp.* **1992**, *26*, 497.
(19) Michels, H. H.; Montgomery, J. A. *J. Phys. Chem.* **1993**, *97*, 6602.
(20) Mebel, A. M.; Lin, M. C.; Morokuma, K.; Melius, C. F. *J. Phys. Chem.* **1995**, *99*, 6842.
(21) Schmitt, R. J.; Krempp, M.; Bierbaum, V. M. *Int. J. Mass Spectrom. Ion Processes* **1992**, *117*, 621.
(22) Barlow, S. E.; Bierbaum, V. M. *J. Phys. Chem.* **1990**, *92*, 3442.
(23) Lias, S. G.; Bartmess, J. E.; Liebman, J. F.; Holmes, J. L.; Levin, R. D.; Mallard, W. G. *J. Phys. Chem. Ref. Data* **1988**, *17*, Suppl. 1.
(24) *Eighth Peak Index of Mass Spectra*; (The Royal Society of Chemistry: London, 1983; Vol. 3, Part 1.
(25) Rozman, B. Yu. *Zh. Prikl. Khim. S.-Peterburg* **1958**, *31* (7), 1101.
(26) Dobychin, S. L.; Smirnov, V. M. *Zh. Prikl. Khim.* S.-Peterburg **1963**, *36* (1), 215.
(27) Vyazovkin, S. *Int. J. Chem. Kinet*. **1996**, *28*, 95.
(28) Vyazovkin, S.; Linert, W. *Chem. Phys.* **1995**, *193*, 109.